Singular coordinate sections of the conic umbilic catastrophes

1982 J. Phys. A: Math. Gen. 15 3057

(http://iopscience.iop.org/0305-4470/15/10/012)

J. Phys. A: Math. Gen. **15** (1982) 3057–3071. Printed in Great Britain

Singular coordinate sections of the conic umbilic catastrophes

F J Wright†, G Dangelmayr‡ and D Lang‡

Institut für Informationsverarbeitung, Universität Tübingen, Köstlinstraße 6, D-7400 Tübingen 1, West Germany

Received 25 September 1981, in final form 14 April 1982

Abstract. We study the intersection of a normal form for the conic umbilic catastrophe of *general* codimension K with planes in control space having all but two control variables set to zero, and display in a set of figures and a table the *geometry* in which strata of the bifurcation set intersect these planes, and the *singularity types* occurring on them. Five distinct curve forms arise. We compare these sections with those of the cuspoids and discuss their occurrence as optical caustics.

1. Introduction

This paper analyses the way in which a normal form for the conic umbilic catastrophe of *general* codimension K (Thom 1972, Zeeman 1977, Poston and Stewart 1978, Gilmore 1981) is intersected by a particular orthogonal set of planes passing through the main singularity. These planes are specified by setting all but two of the control (unfolding) variables equal to zero; hence we call these sections *singular coordinate sections*.

The applications we have in mind are primarily to caustics in optical (and other) wavefields: bifurcation sets of elementary catastrophes manifest themselves as caustics in the short-wavelength limit (Berry and Upstill 1980). However, the singular coordinate sections also provide a reference against which to check any more complete analysis of a specific catastrophe, and a possible basis from which to proceed.

This paper is a sequel to a similar analysis of the infinite sequence of cuspoid catastrophes by Wright (1981), henceforth referred to as I. Callahan (1977) has discussed a related and complementary approach.

The control space of a catastrophe is stratified into submanifolds (strata) within each of which the catastrophe displays a uniform type of singularity (or is non-singular). This leads to a hierarchical *subordination structure* of catastrophes. The union of all submanifolds in which the catastrophe is singular is the bifurcation set $\mathcal{B}$. We determine the *geometry* of the intersection of each stratum of $\mathcal{B}$, identified by its *singularity type*, with each singular coordinate plane.

Special sections of a catastrophe are not necessarily stable in the way that the whole catastrophe is: familiar examples are the so-called beak-to-beak and lips events

† Visiting fellow of the Alexander von Humboldt Foundation. Permanent address: Department of Applied Mathematics, Queen Mary College, London University, Mile End Road, London E1 4NS, UK.

‡ Supported in part by the Volkswagen Foundation of West Germany.

0305-4470/82/103057+15$02.00

(e.g. see Berry and Upstill 1980). The structural stability of sections of catastrophes is discussed in a separate paper (Wright and Dangelmayr 1982, henceforth referred to as II), with particular reference to the stability of specific strata of the singular coordinate sections of the cuspoid and conic umbilic catastrophes. This stability analysis provides information about a *neighbourhood* of the plane of section, on which a more extensive perturbation analysis could be based.

In the next section we introduce the conic umbilic catastrophes in more detail and discuss their subordination structure. All strata branch from the origin, so that a suitable choice of normal form results in the singular coordinate sections of strata having simple semi-algebraic expressions in terms of *single* monomials. This facilitates the simple classification given in § 3 of the curve types in which $\mathscr{B}$ intersects singular coordinate planes. In § 4 we describe how the equations of the intersections may be found, giving a specific example in appendix 1. Section 5 presents the results in a set of figures and a table, which are discussed in § 6 and compared in § 7 with the results found in I for the cuspoids. A discussion of potential physical applications, with particular reference to optics, constitutes the final section.

2. The conic umbilic catastrophes

The cuspoids and conic umbilics together constitute 'almost all' of the simple (non-modal) catastrophes (Arnol'd 1974, reviewed by Gilmore 1981), which consist of:

(a) cuspoids A_k, $k \geq 2$—corank 1;
(b) conic umbilics D_k, $k \geq 4$—corank 2;
(c) exceptional umbilics E_6, E_7, E_8—corank 2.

The symbolism is due to Arnol'd (1973), who classified singularities of complex function-germs. By *catastrophe* we shall mean the restriction to real variables of the unfolding of such a singularity, in which case the number of distinct singularities increases. However, we shall not distinguish dual catastrophes, which differ trivially by the overall sign of the function, since they have the same bifurcation geometry, and the distinction is irrelevant to optics.

The name 'conic umbilic' was coined (by Poston and Stewart 1978, p118) because the sequence is based on Thom's familiar elliptic, hyperbolic ($D_4^{\pm}$) and parabolic (D_5) umbilics. It consists respectively of the higher elliptic and hyperbolic umbilics D_k^- and D_k^+ with k even ≥ 4, which are distinct *catastrophes* although they are equivalent under complex transformations, and the higher parabolic umbilics D_k with k odd ≥ 5. For convenience, we group these catastrophes together as $D_k^{\pm}$ with $k \geq 4$, and understand that only the + sign is to be used when k is odd.

The subscript k is the *multiplicity*—the maximum number of critical points involved in the catastrophe. The codimension $(k-1)$ of the singularity gives the minimum number of control parameters necessary to fully unfold the degenerate critical point, and precisely this number of control variables appears in the normal form. Singularities of lower codimension appear in the unfolding of a given singularity, and in this way a catastrophe *organises* subordinate catastrophes. This subordination structure ties catastrophes together, as shown for the simple catastrophes in figure 1: a catastrophe organises all those which can be reached by following the arrows running from it. (For subordination diagrams distinguishing duals see, for example, Callahan (1978, 1980).)

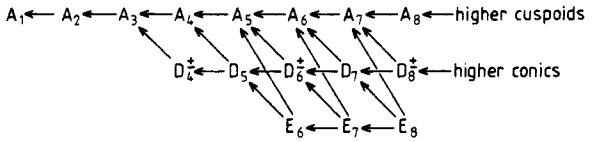

Figure 1. Subordination structure of the simple catastrophes.

The choice of monomials in the cuspoid normal forms is unique, but this is not so for any other catastrophes. We take a set of normal forms which follow a consistent pattern through the whole sequence of higher conic umbilics. These are as given by Poston and Stewart (1978) and Callahan (1977), but the constants are chosen to simplify the subsequent algebra, as is normally done for the cuspoids. Following the notation of I, we represent the codimension-K conic umbilic catastrophe $\mathrm{D}^{\pm}_{K+1}$ by the normal form

$$\phi(s;c)=s_1^2 s_2 \pm s_2^K/K+\sum_{n=4}^{K} c_n s_2^{n-2}/(n-2)+\tfrac{1}{2}c_3 s_1^2+c_2 s_2+c_1 s_1 \qquad (1)$$

where if K is even the + sign only is taken. We shall always use $K(\geqslant 3)$ specifically for the codimension of the catastrophe whose sections we are analysing. For each catastrophe, $\phi(s;c)$ represents a family of functions of the *state variables* $s\equiv(s_1,s_2)$, parametrised by the *control variables* $c\equiv(c_1,c_2,\ldots,c_K)$. The bifurcation set $\mathscr{B}$ is the set of points c at which ϕ has degenerate critical points.

Note that for $K=3$, (1) does not give the more symmetrical normal forms used by Thom (1972) for the first elliptic and hyperbolic umbilics, so that care is required in relating our results to the familiar bifurcation geometry of these catastrophes (in fact, our normal forms give more interesting singular sections). We return to this point in § 6.

3. Classification of the curve types

The intersections occur in five basic forms of curve, which may be generated from a fundamental branch in the positive quadrant whose equation, taking (x, y) as standard coordinates in $\mathbb{R}^2$, is

$$y=x^{\alpha}, \qquad \alpha\geqslant 1, \qquad x\geqslant 0.$$

The *end* Eα is this curve alone, which ends at the origin.

The *bend* Bα is the union of Eα and its reflection in the y axis.

The *cusp* Cα is the union of Eα and its reflection in the x axis.

The *kink* Kα is the union of Eα and its inversion in the origin.

The *hourglass* Hα is the union of all the above forms—it has a branch in every quadrant.

These five forms are illustrated in figure 2.

Only rational values of α can occur, because the curves are all derived from polynomial normal forms. When $\alpha\neq 1$ the fundamental branch has zero slope at the origin (in the limit as $x\to 0$ from above) and the five curve forms are distinct and all have continuous slope. When $\alpha=1$ it is convenient to retain the above notation,

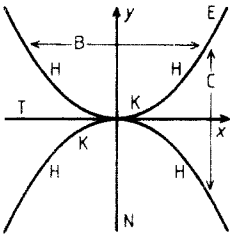

Figure 2. The curve forms. The fundamental, labelled E, is $y = x^{\alpha}$ with $x \geq 0$ and $\alpha > 1$.

although the fundamental branch now has unit slope (everywhere). Then B1 and C1 both represent a *corner*, with *discontinuous* slope at the origin, and H1 represents the intersection of two infinite straight lines. (E1 does not occur in our conic sections.)

In all cases, the three sets {E}, {B, C, K} and {H} may be distinguished by homeotype since they have respectively 1, 2 and 4 branches emanating from the origin. If $\alpha > 1$ then E, B, C, K may be distinguished by an index indicating the angle of rotation of the tangent along the length of the curve (see I), although care is needed with C. The curve forms cannot be classified by diffeotype, since two curves of the same form with different α are not diffeomorphic at the origin.

The curves may occur in combination with the tangent at the origin (the x axis) and the normal at the origin (the y axis), which we indicate by suffixing the curve type by T and N respectively. Of course, when $\alpha = 1$, T and N are not tangents or normals and are consequently not distinct, but we use the same notation for convenience by regarding $\alpha = 1$ as the limit $\alpha \to 1$. In this way we get the types C1T $\equiv$ B1N and H1T $\equiv$ H1N (equivalent by renaming axes), of which we use only the names C1T and H1T by convention. In fact, only ten of the possible combinations occur, namely ET; B, BT, BN, BTN; CT; KT, KTN; HT, HN.

As one would expect, every curve has some kind of singularity at the origin, which is the main singularity of the catastrophe. Any curve which would otherwise be regular, such as B2 or K3, only occurs with T or N. Therefore, there is no significance in α being an integer (other than 1). We shall find that an isolated point and an isolated straight line may also occur.

In the figures in § 5, what we have here called the x axis may lie in either direction along either axis. The scaling of the axes is also arbitrary since we are concerned only with the 'shape' of the curves. Finally, let us define the *form* of a section to be its letter classiffication only (e.g. BTN), and its *type* to be the full symbol complete with its α value (e.g. BαTN).

4. Calculation of the singular coordinate sections of $\mathscr{B}$

We describe here in general terms how to find the equation, in parametric form, of a singular coordinate section of $\mathscr{B}$, and hence the *type of curve* appearing. We then explain how we find the *type of singularity* occurring at each point of $\mathscr{B}$ in the section; these singularities are subordinates of the catastrophe that we are analysing (see figure 1). An example calculation appears in appendix 1.

The bifurcation set $\mathscr{B}$ is the set of points in control space at which $\phi(s; c)$, given by (1), has degenerate critical points. Denoting $\partial\phi/\partial s_i$ by ϕ_i etc, the critical points of

ϕ satisfy

$$\phi_1(s;c) \equiv 2s_1s_2 + c_3s_1 + c_1 = 0, \tag{2a}$$

$$\phi_2(s;c) \equiv s_1^2 \pm s_2^{K-1} + \sum_{n=4}^{K} c_n s_2^{n-3} + c_2 = 0. \tag{2b}$$

They are degenerate when the Hessian matrix $H \equiv \{\phi_{ij}\}$ is singular, i.e. when $\mathcal{H} \equiv \det(H) = 0$. Since

$$\phi_{11}(s;c) \equiv 2s_2 + c_3, \qquad \phi_{12}(s;c) \equiv 2s_1, \tag{3a, b}$$

$$\phi_{22}(s;c) \equiv \pm(K-1)s_2^{K-2} + \sum_{n=4}^{K} c_n(n-3)s_2^{n-4}, \tag{3c}$$

this requires

$$\mathcal{H} \equiv (2s_2 + c_3)\left(\pm(K-1)s_2^{K-2} + \sum_{n=4}^{K} c_n(n-3)s_2^{n-4}\right) - 4s_1^2 = 0. \tag{4}$$

The equation of $\mathcal{B}$ is found, in principle, by eliminating s_1 and s_2 among (2*a*), (2*b*) and (4). This is generally impossible, and even in the singular coordinate sections, where it is possible, it is much simpler, because of their multi-branched nature, to express the sections of $\mathcal{B}$ parametrically (in terms of s_2) as in I.

Note that (2*b*) and (4) depend on s_1 only through s_1^2, and are independent of c_1. Writing (2*a*) as

$$(2s_2 + c_3)s_1 = -c_1 \tag{5}$$

we see that the equations for $\mathcal{B}$ are invariant under $s_1 \to -s_1$, $c_1 \to -c_1$; thus $\mathcal{B}$ is always *symmetrical in* c_1. By squaring (5) we can eliminate s_1 from (2*b*) and (4) to give, respectively,

$$(2s_2 + c_3)^2\left(\pm s_2^{K-1} + \sum_{n=4}^{K} c_n s_2^{n-3} + c_2\right) = -c_1^2, \tag{6a}$$

$$\pm[2(K+1)s_2^{K-1} + c_3(K-1)s_2^{K-2}] + \sum_{n=4}^{K} c_n[2(n-1)s_2^{n-3} + c_3(n-3)s_2^{n-4}] + 4c_2 = 0. \tag{6b}$$

Equations (6) do not have any spurious solutions resulting from squaring (5). To find the singular (i, j) section of $\mathcal{B}$, these equations are solved with all c_n other than c_i and c_j set to zero, by considering three classes of sections: those with $c_1 \neq 0$, $c_3 = 0$, those with $c_1 = 0$, $c_3 \neq 0$, and those with $c_1 = c_3 = 0$. The forms of the curves come from the relative signs which c_i and c_j may take, which determines the relative dispositions of the branches. The solutions express c_i and c_j as powers of s_2 and the α-values come from their relative powers.

At each point of these sections of $\mathcal{B}$ we can easily determine the multiplicity k of the singularity, which is the multiplicity of the root of (2) involved. The subordination diagram then tells us that the singularity must be of type A_k or D_k, and these are distinguished by having respectively corank 1 or 2, i.e. the rank of H is respectively 1 or 0. Therefore, if $\phi_{11} = \phi_{12} = \phi_{22} = 0$ the singularity is D_k, otherwise it is A_k. The only way of distinguishing D_k^+ and D_k^- is by examining the local form of ϕ, as discussed, for example, by Poston and Stewart (1978) (see also II).

Three non-trivial types of solution for c_i and c_j arise: curve segments on which s_1, $s_2 \neq 0$; curve segments on which $s_1 = 0$, $s_2 \neq 0$; line segments and plane regions on which $s_1 = s_2 = 0$. These are mutually exclusive and *always exclude the origin*, where the solution of equations (6) for s is maximally degenerate. The distinction is needed for the local analysis necessary to distinguish $D_k^{\pm}$ and for the stability analysis discussed in II. A more important distinction for our present purposes is whether or not s_1 and s_2 may take either sign, which corresponds to the simultaneous occurrence of singularities at $\pm s$ with the same c-value (see appendix 1). Geometrically this corresponds to a self-intersection of $\mathcal{B}$.

5. Results

We examine the singular (i, j) sections of the codimension-K conic umbilic normal form (1), in which all control variables c_n other than c_i and c_j, with $K \geq i > j \geq 1$, are set to zero. Sections involving c_1, c_2 and c_3 behave differently from the general section, partly because of the way these variables are singled out in the normal form (1), and partly because they are the coefficients of low powers of s_1 and s_2, so that the full singularity structure of the general section does not appear. Even sections involving c_4 do not quite display the general forms, but we can incorporate these into the general classification by using A_1 to represent a non-singular (Morse) function, and using D_3 as a synonym for A_3. (Indeed, (1) with $K = 2$ is equivalent to the normal unfolding of the A_3 singularity; see also Callahan (1977).)

It suffices to distinguish seven classes of sections, which in 'i, j-order' are: (2, 1); (3, 1);$(i \geq 4, 1)$;(3, 2);$(i \geq 4, 2)$;$(i \geq 4, 3)$; and (i, j) with $i > j \geq 4$, the general section. We shall use e, h, p(i, j) to mean respectively the (i, j) section of an elliptic, hyperbolic or parabolic umbilic. We display the general structure of these classes of sections in figures 3–9, which show only the *form* of the intersections with $\mathcal{B}$, but are valid for

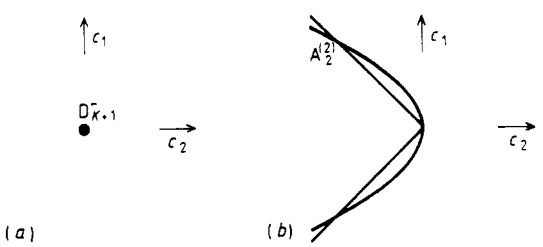

Figure 3. (2, 1) sections: (*a*) elliptic; (*b*) limiting hyperbolic and parabolic: V shape for $K = 3$ and parabola as $K \to \infty$.

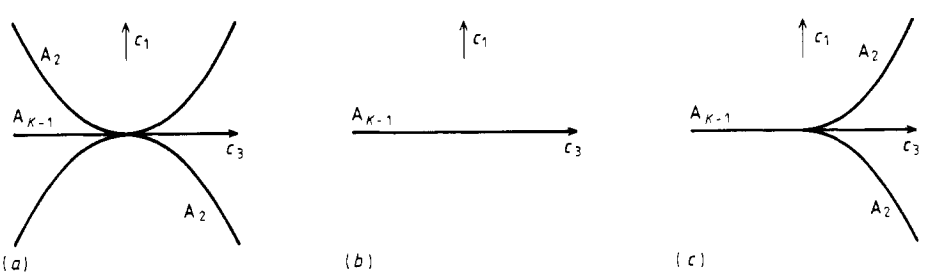

Figure 4. (3, 1) sections: (*a*) elliptic; (*b*) hyperbolic; (*c*) parabolic.

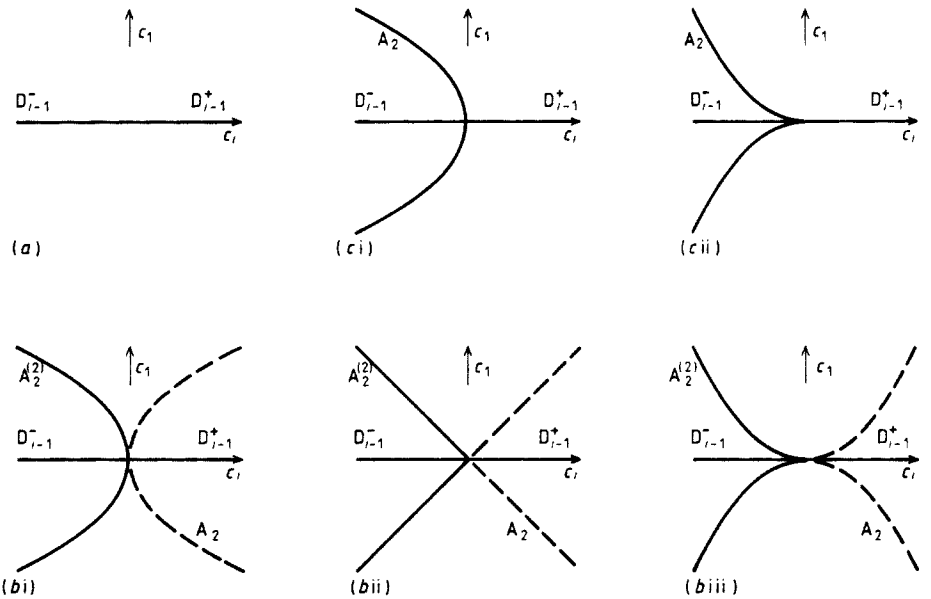

Figure 5. ($i \geq 4$, 1) sections: (a) elliptic: (b) hyperbolic—broken branches included if i is even—(i) $i < \frac{1}{2}(K+3)$, (ii) $i = \frac{1}{2}(K+3)$, (iii) $i > \frac{1}{2}(K+3)$; (c) parabolic—(i) $i < \frac{1}{2}(K+3)$, (ii) $i > \frac{1}{2}(K+3)$.

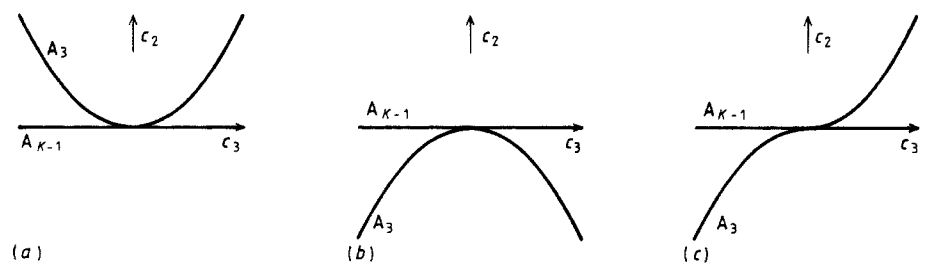

Figure 6. (3, 2) sections: (a) elliptic; (b) hyperbolic; (c) parabolic.

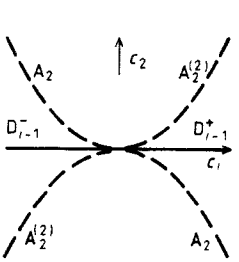

Figure 7. ($i \geq 4$, 2) sections—schematic. One broken branch will occur for K, i both odd, two otherwise (see table 1).

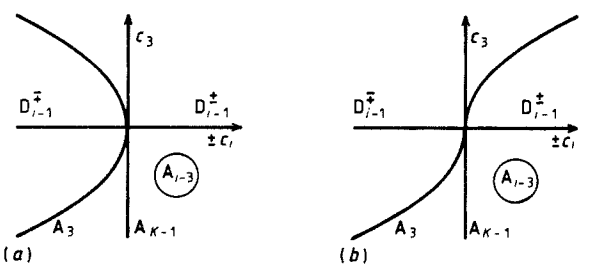

Figure 8. ($i \geq 4$, 3) sections: (a) K, i both odd or both even; (b) otherwise. Upper signs for hyperbolic and parabolic, lower signs for elliptic.

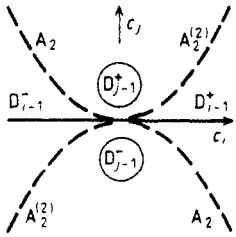

Figure 9. $(i, j \geq 4)$ section—schematic. One or two broken branches will occur, depending on i, j, K (see table 1).

all K. The *type* of the intersections is given explicitly in table 1 for $3 \leq K \leq 9$, along with the general expressions for α which allow the table to be easily extended to any desired K. We always plot the c_i axis horizontally and the c_j axis vertically, with $i > j$. The figures are schematic and do not generally correspond to any particular α-values. The full branches always occur; the broken branches in some of the figures representing a class of sections may occur, depending upon the particular section within the class.

Each curve and line is labelled with the singularity (using Arnol'd's notation) occurring on it which, from the subordination diagram in figure 1, is either A_k or $D_k^{\pm}$ with $k < K+1$. The origin is *always* a $D^{\pm}_{K+1}$ point, of course, but is only labelled as

Table 1. Classification of curve types in singular (i, j)-sections. A + or − sign in column 2 means that the classification relates only to D^+_{even} or D^-_{even} respectively, as well as to D_{odd}.

			Name of catastrophe Codimension K						
i, j	±	α	$D_4^{\pm}$ 3	D_5 4	$D_6^{\pm}$ 5	D_7 6	$D_8^{\pm}$ 7	D_9 8	$D_{10}^{\pm}$ 9
2, 1	+	$\frac{2(K-1)}{K+1}$	$B^2 1$	$B\frac{6}{5}$	$B^2\frac{4}{3}$	$B\frac{10}{7}$	$B^2\frac{3}{2}$	$B\frac{14}{9}$	$B^2\frac{8}{5}$
3, 1	−	$\frac{1}{2}(K+1)$	H2T	$C\frac{5}{2}T$	H3T	$C\frac{7}{2}T$	H4T	$C\frac{9}{2}T$	H5T
4, 1	+	Greater of		$C\frac{5}{4}T$	H1T	$B\frac{8}{7}N$	$H\frac{5}{4}N$	$B\frac{4}{3}N$	$H\frac{7}{5}N$
5, 1	+	$\frac{K+1}{2(K-i+2)}$			$C^2\frac{3}{2}T$	$C\frac{7}{6}T$	$C^2 1T$	$B\frac{10}{9}N$	$B^2\frac{6}{5}N$
6, 1	+					$C\frac{7}{4}T$	$H\frac{4}{3}T$	$C\frac{9}{8}T$	H1T
7, 1	+	and					$C^2 2T$	$C\frac{3}{2}T$	$C^2\frac{5}{4}T$
8, 1	+							$C\frac{9}{4}T$	$H\frac{5}{3}T$
9, 1	+	$\frac{2(K-i+2)}{K+1}$							$C^2\frac{5}{2}T$
3, 2		$K-1$	B2T	K3T	B4T	K5T	B6T	K7T	B8T
4, 2				$C\frac{3}{2}T$	$B\frac{4}{3}T$	$C\frac{5}{4}T$	$B\frac{6}{5}T$	$C\frac{7}{6}T$	$B\frac{8}{7}T$
5, 2					$E^2 2T$	$K\frac{5}{3}T$	$E^2\frac{3}{2}T$	$K\frac{7}{5}T$	$E^2\frac{4}{3}T$
6, 2		$\frac{K-1}{K-i+2}$				$C\frac{5}{2}T$	B2T	$C\frac{7}{4}T$	$B\frac{8}{5}T$
7, 2							$E^2 3T$	$K\frac{7}{8}T$	$E^2 2T$
8, 2								$C\frac{7}{2}T$	$B\frac{8}{3}T$
9, 2									$E^2 4T$

Table 1 continued.

			Name of catastrophe Codimension K						
i, j	$\pm$	α	$D_4^{\pm}$ 3	D_5 4	$D_6^{\pm}$ 5	D_7 6	$D_8^{\pm}$ 7	D_9 8	$D_{10}^{\pm}$ 9
4, 3			↑	B2TN	K3TN	B4TN	K5TN	B6TN	K7TN
5, 3					B2TN	K3TN	B4TN	K5TN	B6TN
6, 3		$K-i+2$	plus			B2TN	K3TN	B4TN	K5TN
7, 3			plane				B2TN	K3TN	B4TN
8, 3								B2TN	K3TN
9, 3									B2TN
5, 4					C_2^3T	B_3^4T	C_4^5T	B_5^6T	C_6^7T
6, 4						$E^2 2T$	K_3^5T	$E^2\,{}_2^3T$	K_5^7T
7, 4		$\frac{K-j+2}{K-i+2}$	plus				C_2^5T	B2T	C_2^7T
8, 4			plane					$E^2 3T$	K_3^7T
9, 4									C_2^7T
6, 5						C_2^3T	B_3^4T	C_4^5T	B_5^6T
7, 5		$\frac{K-j+2}{K-i+2}$	plus				$E^2 2T$	K_3^5T	$E^2\,{}_2^3T$
8, 5			plane					C_2^5T	B2T
9, 5									$E^2 3T$
7, 6							C_2^3T	B_3^4T	C_4^5T
8, 6		$\frac{K-j+2}{K-i+2}$	plus					$E^2 2T$	K_3^4T
9, 6			plane						C_2^5T
8, 7		$\frac{K-j+2}{K-i+2}$	plus					C_2^3T	B_3^4T
9, 7			plane						$E^2 2T$
9, 8		$\frac{K-j+2}{K-i+2}$	plus						C_2^3T
			plane						

such in figure 3(a), since e(2, 1) is the only section in which the origin is the only singular point. In the higher-order sections ($i \geqslant 5, j \geqslant 3$) every point of the plane is singular, and we indicate this in table 1, and in the figures by putting the symbol for the singularity in a circle. For $j \geqslant 5$, the singularity is of type $D_{j-1}^{\mathrm{sign}(c_j)}$, otherwise it is A_k (for some k) over the whole plane. Note that the (4, 3) plane is not contained in $\mathscr{B}$ because A_1 is non-singular, although a cursory glance at figure 8 might suggest that it is.

The symbol A_2^2 represents the intersection of two A_2-strata of $\mathscr{B}$, which is familiar in the swallowtail and first hyperbolic umbilic. The A_2^2 singularity involves two pairs of coincident critical points, and occurs in codimension 2, whereas four critical points coalesce generically only in codimension 3. No other self-intersections of $\mathscr{B}$ occur in singular coordinate sections of our normal forms. The symbol which actually appears in the figures is $A_2^{(2)}$, which means that the curve may be either A_2 or A_2^2, depending on the particular section within the class. The two cases are distinguished in table 1 by adding a superscript 2 to the curve-form letter if the curve is a self-intersection, e.g. E^2.

The (2, 1) and ($i \geq 4$, 1) sections of elliptic umbilics and the (3, 1) sections of hyperbolic umbilics possess no *curved* branch and so cannot be classified in table 1. A + or − sign appearing in the column headed ± means that for k even this section applies only to D_k^+ (hyperbolic) or to D_k^- (elliptic) respectively. The sequence of α-values follows a fairly clear pattern through table 1, except that our classification convention requires $\alpha \geq 1$. Consequently there is a reversal in the progression of α-values as α passes through 1, which happens only in the ($i \geq 4$, 1) section of the table, and is accompanied by the sections changing from BαN to CαT and from HαN to HαT. When $\alpha = 1$, the naming convention is slightly ambiguous, as discussed in § 3.

6. Discussion of the results

We expect the most significant groupings of sections to depend on whether they involve c_1 or c_3, because these are the only controls multiplying powers of s_1 in the normal form (1). Therefore, we expect the classes of sections (2, 1) and ($i \geq 4$, 1) not involving c_3; (3, 2) and ($i \geq 4$, 3) not involving c_1; ($i \geq 4$, 2) and (i, j) with $i > j \geq 4$, not involving either c_1 or c_3, to be closely related. The figures and table 1 show that this is the case: (2, 1) is as ($i \geq 4$, 1) but without the T or N line along the c_i axis; (3, 2) is as ($i \geq 4$, 3) but without the N line along the c_i axis and without the plane of singularities which occurs for $i \geq 5$; and ($i \geq 4$, 2) is as the general section but without the plane of singularities.

Self-consistency requires that each axis should always display the same singularity irrespective of the section in which it appears; that this is so is readily confirmed from the figures which show that every point of an axis, excluding the origin, displays the following singularity:

axis	:	c_1, c_2	c_3	c_4	$c_n, n \geq 5$
singularity	:	non-singular	A_{K-1}	A_3	D_{n-1}

(the last case is by virtue of the axis lying in a plane of D_{j-1} singularities if it is a c_j axis). One advantage of our analysis is that it finds all these axial lines which are essential parts of $\mathcal{B}$, whether or not they are stable. It is very difficult to find unstable features numerically, as discussed further in I.

It is instructive to relate our general classification to Thom's familiar hyperbolic and elliptic umbilics $D_4^{\pm}$, and to determine which of their characteristic features are also characteristic of the higher conic umbilics. Figure 3(a) shows that the isolated point at the origin of the (2, 1) section is indeed a characteristic of *all* elliptic umbilics. However, figure 3(b) together with table 1 shows that the characteristic *corner* of the (2, 1) section of D_4^+ is peculiar to this catastrophe, and this section of all higher hyperbolic and parabolic umbilics has continuous slope.

We note that (2, 1) sections are the only sections not garnished with axial lines, related to which is the fact that these are the only sections in which $\alpha = 2(K-1)/(K+1)$ is never an integer, other than 1 when $K = 3$—if it were then the curve would not be singular at the origin, as discussed in the penultimate paragraph of § 3. As K increases from 3 towards ∞, α increases from 1 towards 2, thereby defining the two *limiting curve types* shown in figure 3(b) for the h, p(2, 1) sections of $\mathcal{B}$. The nature of the singular (2, 1) section of the general conic umbilic (including D_3!), and especially the origin of the A_2^2 curves, is admirably illustrated in figure 33 of Callahan (1977). (He also studies the general (2, 1) sections of $D_4^{\pm}$, D_5 and $D_6^{\pm}$.)

Stability of the intersections is discussed in detail in II, but a few observations concerning stability are appropriate here. The hourglass curve in the (3, 1) section of D_4^- results from cutting longitudinally through the cusped triangular cone shape of $\mathcal{B}$, and apart from the origin its *branches* are therefore stable. The shape of the hourglass curve is the same as that of a beak-to-beak event, which occurs in a section tangent to a rib (cusped edge) with a particular configuration and is a special case of a cusp catastrophe, rather than a distinct type of singularity. The hourglass in the (3, 1) section of D_4^- may be regarded as a degenerate beak-to-beak, in which it coincides with a higher singularity, and in principle the (3,1) section of D_4^+ may be regarded as a degenerate lips event which is not visible. In fact, many of our singular sections may be regarded as such 'degenerate concatenations' (see also Callahan 1977).

The A_2 line along the c_3 axis in the (3, 1) sections of $D_4^\pm$ results from a *tangency* of the A_2 stratum of $\mathcal{B}$ with the plane of section, and is consequently *unstable*. The global existence of this line is an artifact of our choice of normal forms—if the unfolding monomial s_1^2 in (1) is replaced by $(s_1^2+s_2^2)$ to give the more symmetrical unfolding of D_4^- used by Thom (1972) and Berry *et al* (1979), and its analogue for D_4^+, then this sheet of the A_2 stratum curves out of the (3, 1) plane away from the origin. In the (3, 2) plane of $D_4^\pm$, however, the A_2 line along the c_3 axis results from an *intersection* with $\mathcal{B}$, and is consequently *stable*. With the more symmetrical normal forms the A_2 line curves quadratically in the opposite direction to the quadratic A_3 curve. The A_3 curve itself is completely unstable and small perturbations will unfold it into one or three A_2 curves, although it cannot disappear completely.

Table 1 shows that E curves can only occur as self-intersections of $\mathcal{B}$ (A_2^2 singularities), but in h(2, 1) and h($i \geqslant 4$, 1) sections C and B curves also occur as self-intersections. Such self-intersection curves may be regarded as curves which have 'doubled back' on themselves. This interpretation is consistent with the singularity type being A_2^2, and with the alternations down some of the columns of table 1 between E^2 and B, and between C^2 or B^2 and H as illustrated in figure 5.

Our results for $K \geqslant 4$ are completely consistent with those of Godwin (1971), Woodcock and Poston (1974) and Callahan (1977).

7. Comparison with the cuspoids

The singular coordinate sections of cuspoid catastrophes display a subset of the features displayed by the conics. Specifically, the following do not occur for the cuspoids: hourglass curves (H), isolated points, isolated axial lines and normal lines (N)—for the cuspoids axial lines occur only as tangents (T). The case $\alpha = 1$ does not occur for cuspoids, and for B, C and K the values of α (which are always rational) are restricted to the forms even/odd, odd/even and odd/odd respectively. For the cuspoids, self-intersections occur only on E, and not on C or B; however, a cusp (C) can occur alone whereas for the conics it is *always* accompanied by the tangent (as CT).

There is an extremely close analogy, which we investigate in detail in appendix 2, between the conic sections with $c_1 = c_3 = 0$ and the cuspoids. This is because with $c_1 = c_3 = 0$, if it were not for the term $s_1^2 s_2$, the normal form (1) would be a cuspoid normal form (see also Callahan 1977). The ($i \geqslant 4$, 2) conic sections are analogous to the ($i \geqslant 4$, 3) cuspoid sections, discussed in I, and the (i, j) sections of the conics and cuspoids are analogous to each other for $i > j \geqslant 4$. The $D_k^\pm$ points in the conic sections are analogous to the A_k points in the cuspoid sections. The only difference is that

the $(i \geqslant 4, 2)$ conic sections are not singular planes, whereas the $(i \geqslant 4, 3)$ cuspoid sections are A_2 planes. In fact, in both the cuspoid and the conic singular sections, planes of singularities occur only if $j \geqslant 3$.

Consequently the general conic sections have exactly the same classifications as the cuspoid sections, so that the bottom of table 1 ($j \geqslant 4$) is equivalent to a reorganised version of the bottom left corner of table 2 of I (restricted to $i > j \geqslant 4$, which implies $K \geqslant 5$). With the particular choices of normal forms made here and in I, the equations of these matching sections are *identical*, except that elliptic sections are inverted in the origin $(c \to -c)$ relative to cuspoid sections.

8. Applications

In physical applications singular coordinate sections are not quite as special as they appear. Any experimentally determined bifurcation sets will be blurred to some degree, either as an unavoidable consequence of the physics (diffraction blurring of optical caustics, thermal fluctuations, noise etc) or simply as a result of experimental error. This will have the effect of stabilising non-generic phenomena. Therefore one *can* expect to find singular sections, including their less stable features, to 'within experimental error'.

This is well illustrated by optical experiments. In a study of 'optical caustics in the near-field from liquid drops' Nye (1978) found typically 'several tens of elliptic umbilic catastrophes' which all focused in the same plane. In our notation this focal plane is the singular (2, 1) section of D_4^-, which is *completely* unstable (see II). Nye (1978, p 26) observes that: 'The cusped triangle is a non-singular section of an elliptic umbilic, but its star-shaped diffraction pattern (Trinkaus and Drepper 1977; Berry, Nye and Wright 1979) is hard to distinguish from the pattern from a singular section; thus one has the erroneous impression that an elliptic umbilic singularity has already been formed.'

Using 'liquid drops under gravity' Nye (1979) has observed the diffraction patterns of caustics indistinguishable from singular (2, 1) sections of D_4^+ and D_5. These two can only be distinguished by very subtle details of their diffraction patterns, and one would imagine from Nye's photographs (figures 4(d) and 8(f)) that the caustics were both corners. In fact, as we have already remarked, only D_4^+ displays a corner (B1) whereas D_5 displays a B_5^6 with continuous slope (as plotted in figure 1(b) of I), although the difference is hard to see.

As an illustration of optical applications of our classification, let us see to what extent it enables us to deduce that figure 8(f) of Nye (1979) is a singular (2, 1) section of D_5. The photograph is clearly close to some singular section. In principle, it is possible to observe a section arbitrarily close to any particular singular section. However, an empirical consequence of the symmetry of a typical experimental arrangement is that frequently the 'optical axis' or 'focusing direction' of the system coincides with a control space axis of the normal form, which implies that observed sections of the caustic are locally coordinate sections. This is implicit in much of catastrophe optics, and we assume it to be the case here.

A section containing a plane of singularities could only appear on a screen if it were placed parallel to the beam, i.e. at glancing incidence, which is rarely the case. It is certainly not possible in Nye's optical system, thereby immediately ruling out most sections of both the conics and the cuspoids. Noting that Nye's photograph

displays no signs of T or N lines further rules out, among the conics and cuspoids, all but (2, 1) sections. In fact, it is well known in catastrophe optics that these are the most frequently observed sections of caustics (see, for example, Berry and Upstill 1980).

Let us assume that we know, perhaps from the general form of neighbouring sections, that we are dealing with a conic umbilic. The curve clearly has α close to 1. The effects of small perturbations should show that the curve is completely stable, so it is $B\alpha$, not $B^2\alpha$. Then from table 1 the curve is most likely to be the B_5^6 resulting from a (2, 1) section of D_5, since this catastrophe has the lowest possible codimension.

This optical example shows that our catalogue of singular coordinate sections provides at least useful corroborative evidence for the assignment of sections of bifurcation sets. It also provides consistency checks on any more extensive studies of particular catastrophes, such as Godwin's (1971) exhaustive study of D_5.

For applications to optics, the next stage of this program is to evaluate the diffraction catastrophes for the singular coordinate sections, for which the present detailed study of the caustics is an essential precursor. However, it is most unlikely that a concise classification of the sort presented here would be possible for the diffraction patterns.

Acknowledgments

FJW thanks the Alexander von Humboldt Foundation for a research fellowship, and Professor W Güttinger and the members of his institute for their hospitality during its tenure. We are also grateful to Dieter Armbruster and Colin Upstill for their comments on the manuscript.

Appendix 1. An example calculation.

As an illustration, let us consider the family of sections ($i \geq 4$, 1), in some ways the most complicated. They display all features except a singular plane. Equations (6) become

$$4s_2^2(\pm s_2^{K-1} + c_i s_2^{i-3}) = -c_1^2 \qquad \pm(K+1)s_2^{K-1} + c_i(i-1)s_2^{i-3} = 0. \qquad \text{(A1.1}a, b\text{)}$$

Since $i \geq 4$, $s_2 = 0$ is a root of (A1.1b), and if $c_1 = 0$ it is also a root of (A1.1a). Therefore the c_i axis is part of $\mathcal{B}$. From (2), the root also has $s_1 = 0$, and has multiplicity $(i-1)$. From (3), $\phi_{11} = \phi_{12} = 0$, and $\phi_{22} = 0$ unless $i = 4$. Therefore if $i = 4$, the singularity is A_3, if $i \geq 5$ it is D_{i-1}, i.e. it is a 'generalised D_{i-1}' singularity where $D_3 \equiv A_3$ as discussed in § 5. (A singular plane would arise if $s_2 = 0$ were a multiple root of (A1.1a) for all c_i and c_j.)

Solving (A1.1) for c_i and c_1 gives

$$c_i = \mp\left(\frac{K+1}{i-1}\right)s_2^{K-i+2} \qquad c_1^2 = \pm 4\left(\frac{K-i+2}{i-1}\right)s_2^{K+1}. \qquad \text{(A1.2}a, b\text{)}$$

In the elliptic case K is odd, the lower sign applies and (A1.2b) has no non-trivial solutions—hence figure 5(a) and the + sign in table 1. In the hyperbolic case K is again odd but the upper sign applies and (A1.2b) allows all c_1 and s_2. Now if i is odd, (A1.2a) allows only $c_i \leq 0$, giving only two branches which form a cusp or bend, but if i is even it allows all c_i, giving four branches which form an hourglass curve.

The distinction between cusp and bend (or the orientation of the hourglass) depends on the slope at the origin, i.e. on the relative magnitudes of the powers of s_2 in (A1.2). If $2(K-i+2)>K+1$, $c_i \to 0$ faster than c_1 giving a bend. In the special case when $2(K-i+2)=K+1$, i.e. $i=\frac{1}{2}(K+3)$, we have a corner (labelled $C^2$1T in table 1); otherwise we have a cusp. The exact orientation of the curves is shown in figure 5(*b*). When the curve changes from a cusp to a bend, the c_i axis changes from a tangent to a normal. Note that in the cusp and bend cases both signs of s_2 give the same point on the curve, making these curves self-intersections of $\mathcal{B}$.

The parabolic case has K even and takes the upper sign, so that (A1.2*b*) allows only $s_2 \geqslant 0$. Consequently (A1.2*a*) gives only $c_i \leqslant 0$, as in figure 5(*c*). The result is like the hyperbolic case with odd i, but now s_2 cannot take both signs, so this curve is *not* a self-intersection.

The value of α is given by the greater of $(K+1)/2(K-i+2)$ and $2(K-i+2)/(K+1)$. On the curves, (2*a*) gives a 1 :: 1 relation between s_1 and s_2, and (A1.2) corresponds to a double root of (A1.1*a*) and hence of (2). The Hessian matrix H is non-zero, so we have a curve of A_2 singularities. Therefore, when it is a self-intersection it is A_2^2, and both s_1 and s_2 change sign between the two intersecting sheets of $\mathcal{B}$. Generally, when the expressions for c_i and c_j on a curve are *even* in s_2, then the curve lies in the A_2^2 stratum of $\mathcal{B}$.

Appendix 2. Relation between conic umbilic and cuspoid catastrophes.

We remarked in § 7 on the close analogy between certain conic umbilic and cuspoid singular sections. Here we explore in a little more detail the analogous $(K-2)$-*dimensional subspaces* (rather than just singular sections) of the universal unfoldings of $D_{K+1}^{\pm}$ and A_{K+1} having respectively $c_1=c_3=0$ and $c_1=c_2=0$. For convenience, let us define a slightly modified set of control variables for $D_{K+1}^{\pm}$ by $c_3'=\pm c_2$ and $c_n'=\pm c_n$ for $n \geqslant 4$. Then from (1) we may write the normal form for this partial unfolding of $D_{K+1}^{\pm}$ as

$$\phi(s;c')=s_1^2 s_2 \pm \Big(s_2^K/K + \sum_{n=3}^{K} c_n' s_2^{n-2}/(n-2) \Big).$$

Its critical points satisfy

$$s_1=0 \qquad s_2^{K-1} + \sum_{n=3}^{K} c_n' s_2^{n-3} = 0 \tag{A2.1a}$$

or

$$s_2=0 \qquad s_1^2 \pm c_3' = 0. \tag{A2.1b}$$

Multiple critical points can only occur with $s_1=0$, which is the basis of the analogy.

We choose similar names for the variables in the partial unfolding of A_{K+1}, whose normal form (as used in I) we may write as

$$\Phi(s_2;c')=s_2^{K+2}/(K+2)+\sum_{n=3}^{K} c_n' s_2^n/n.$$

Its critical points may then be written analogously as satisfying

$$s_2^{K-1} + \sum_{n=3}^{K} c_n' s_2^{n-3} = 0 \qquad \text{or} \qquad s_2^2 = 0. \tag{A2.2a, b}$$

The structure of those critical points of ϕ and Φ with $s_2 \neq 0$, given respectively by (A2.1*a*) and (A2.2*a*), is *identical*. If they coalesce (at $s_2 \neq 0$) they both produce *cuspoid* singularities of the same codimension.

The critical points of ϕ and Φ with $s_2 = 0$ behave slightly differently: Φ *always* has a singularity at $s_2 = 0$, but if $c_2 \equiv c_3' \neq 0$ then ϕ does not. Suppose $c_n' = 0$ for all $n < j$, and $c_j' \neq 0$. Then if $j > 3$ the double root of (A2.2*b*) merges with the root of (A2.2*a*) at $s_2 = 0$, giving in general an A_{j-1} singularity of Φ. However, (A2.1*b*) only has a double root if $c_3' = 0$, which merges with the root of (A2.1*a*) at $s_2 = 0$. If $j = 4$, ϕ has an A_3 singularity as does Φ, but if $j > 4$, ϕ has a D_{j-1} singularity (since then $\phi_{11} = \phi_{12} = \phi_{22} = 0$) instead of the A_{j-1} singularity displayed by Φ.

References

Arnol'd V I 1973 *Funct. Anal. Appl.* **6** 254–72

—— 1974 *Usp. Mat. Nauk.* **29** 11–49 (*Russ. Math. Surv.* **29** 10–50)

Berry M V, Nye J F and Wright F J 1979 *Phil. Trans. R. Soc.* A **291** 453–84

Berry M V and Upstill C 1980 *Progress in Optics* vol 18, ed E Wolf (Amsterdam: North-Holland) 257–346

Callahan J 1977 *Am. Math. Mon.* **84** 765–803

—— 1978 *Preprint: Special bifurcations of the double cusp* Mathematics Institute, University of Warwick

—— 1980 *Mathematical modelling* **1** 283–309

Gilmore R 1981 *Catastrophe Theory for Scientists and Engineers* (NewYork: Wiley)

Godwin A N 1971 *Publ. Math. IHES* **40** 117–38

Nye J F 1978 *Proc. R. Soc.* A **361** 21–41

—— 1979 *Phil. Trans. R. Soc.* A **292** 25–44

Poston T and Stewart I N 1978 *Catastrophe Theory and its Applications* (London: Pitman)

Thom R 1972 *Stabilité structurelle et morphogénèse* (Reading, Mass.: Benjamin) (Engl. transl.: *Structural stability and morphogenesis* (Reading, Mass.: Benjamin 1975))

Trinkaus H and Drepper F 1977 *J. Phys. A: Math. Gen.* **10** L11–6

Woodcock A E R and Poston T 1974 *A Geometrical Study of the Elementary Catastrophes* (Berlin: Springer)

Wright F J 1981 *J. Phys. A: Math. Gen.* **14** 1587–99

Wright F J and Dangelmayr G 1982 submitted to *J. Phys.* A

Zeeman E C 1977 *Catastrophe Theory: Selected Papers 1972–1977* (Reading, Mass.: Addison-Wesley)